Influence of finite wavelength on the quantum kicked rotator in the semiclassical regime

James D. Hanson

Institute for Fusion Studies, The University of Texas at Austin, Austin, Texas 78712

Edward Ott and Thomas M. Antonsen, Jr.

Laboratory for Plasma and Fusion Energy Studies, The University of Maryland, College Park, Maryland 20742

(Received 12 August 1983)

The quantum kicked rotator, the classical limit of which is described by the standard map, is considered. Particular attention is devoted to a study of the effect of finite quantum wavelength on the detailed structure of phase space which appears in the classical limit. In the classical case, for large values of the nonlinearity parameter, most of the trajectories are ergodic. However, in addition to these ergodic trajectories, there can be small integrable regions of phase space, known as accelerator modes, which dominate the long-time evolution of the expected value of the particle energy. In this paper it is shown that this behavior is modified in the quantum case for small but finite values of the wavelength (i.e., Planck's constant). A simple model is presented to explain this modification. Based on our results, it is speculated that certain problems in the application of statistical concepts to intrinsically stochastic problems of classical mechanics may, in some cases, be mitigated by quantum effects.

I. INTRODUCTION

Recently, a great deal of effort[1,2] has been devoted to the study of chaos in low-dimensionality Hamiltonian systems (such as those describing the classical motion of a particle). In particular, the transition from integrable to ergodic behavior has been studied,[2,3] along with statistical properties of orbits (e.g., diffusion) in the chaotic regime.[2,4,5] More recently, the connection between classical Hamiltonian systems which display chaotic behavior and their quantum counterparts has begun to receive attention.[6-11] One reason for this interest is that understanding developed in one picture can be used to develop understanding in the other. Another is the desire to understand in what sense the classical solution for a chaotic case is a limit of the corresponding quantum solution as $\hbar$, Planck's constant, is allowed to approach zero. The latter question has important practical (as well as conceptual) implications, since it bears on the question of how good classical and semiclassical approximations to quantum problems are. These questions are not only of interest for quantum mechanics, but are also important for any situation in which it is desired to use a ray approximation to some kind of wave equation, and the ray equations (which are necessarily a Hamiltonian system) yield chaotic solutions (cf., for example, Refs. 12 and 13). Such situations occur very generally in a variety of purely classical problems (e.g., plasma waves[12,13]).

In the quantum case, somewhat of a paradox arises for the situation in which the energy spectrum is discrete (e.g., for a bounded system). In this case, the wave function may be expressed as

$$\psi(\vec{x},t)=\sum_{\alpha} A_{\alpha}\psi_{\alpha}(\vec{x})\exp(-i\omega_{\alpha}t) , \qquad (1a)$$

where $\psi_{\alpha}(\vec{x})$ denotes a normalized eigenfunction of the Schrödinger equation with energy level $E_{\alpha}=\hbar\omega_{\alpha}$. It is argued by some that a wave function of the form in Eq. (1a) (i.e., with a discrete ω_{α} spectrum) cannot be considered to be in any sense chaotic.[14] On the other hand, other researchers argue that there are clear quantum manifestations of classical chaotic behavior for small $\hbar$. These claimed manifestations include[11] such phenomena as extreme sensitivity of the E_{α} to small changes in the Hamiltonian, the form of the eigenfunctions $\psi_{\alpha}(\vec{x})$, and the distribution of energy differences between adjacent energy levels.

A very striking result concerning the relation of classical chaos to the small-$\hbar$ limit of quantum mechanics has been obtained by Casati *et al.*[6] These authors consider a Hamiltonian which involves only one space dimension, but which has a potential which represents periodic impulses kicking the system at time intervals separated by T. In the classical case, this Hamiltonian leads to a discrete-time, two-dimensional map [cf. Eqs. (6) and (7) of Sec. II]. This map, alternatively called the "standard map" or the "Taylor-Chirikov map," has been much studied, and to a certain extent, it has served as a paradigm of how chaos can arise in a simple Hamiltonian system. In particular, if the strength of the impulse kicks is large enough, the momentum variable P behaves diffusively. That is, some suitable average value of P^2 increases linearly with time t. Casati *et al.* considered the quantum version of the same problem and numerically solved for the wave function as a function of time with $\hbar$ small. They found that for early times, the average value of P^2 increased linearly with time at the classical diffusive rate, but that for long time this linear increase slowed and eventually appeared to cease. Since their Hamiltonian is a periodic function of time (rather than being constant in time), Eq. (1a) cannot apply.

HANSON, OTT, AND ANTONSEN

By Floquet's theorem, however, there does exist an analog to Eq. (1a), namely,

$$\psi(\vec{x},t)=\sum_\alpha A_\alpha P_\alpha(\vec{x},t)\exp(-i\omega_\alpha t) , \qquad (1b)$$

where $P_\alpha(\vec{x},t)$ are periodic in t with period T, the period of the impulses. The observed saturation of diffusion is understandable[8,9] if Eq. (1b) applied with discrete "quasienergy levels" $E_\alpha=\hbar\omega_\alpha$, because then Eq. (1b) is almost periodic [i.e., if one waits long enough, $\psi(\vec{x},t)$ will come arbitrarily close to $\psi(\vec{x},0)$]. Recently, Fishman, Grempel, and Prange[10] have presented strong arguments supporting the idea that the quasienergy spectrum of the system studied by Casati et al. is discrete. To see why the classical diffusive result might apply initially, let $\Delta\omega$ denote a typical spacing between adjacent ω_α eigenvalues, and note that for $(\Delta\omega)t \lesssim 1$ the wave function $\psi(\vec{x},t)$ does not yet "know" that the spectrum is discrete. Furthermore, if $\Delta\omega$ decreases with $\hbar$, then the duration of the initial interval over which P diffuses approaches infinity as $\hbar$ approaches zero.

In this paper we study the problem of Casati et al. (henceforth called the *kicked rotator*) for small finite $\hbar$ and "short" times, $(\Delta\omega)t \lesssim 1$, i.e., over the time interval in which the closest correspondence between quantum and classical time-evolution behavior is expected. Even in this time interval, we find that significant differences in statistical behavior may occur between the quantum and classical kicked-rotator problems. These differences result from small integrable regions of phase space in the classical problem. Such integrable regions, called *accelerator modes*, occur only in narrow parameter ranges of the kicking strength, and did not apply to the numerical experiments of Casati et al. In the classical case, particles initially falling in the region of the accelerator mode experience acceleration rather than diffusion (cf. Sec. II). Thus, if a small fraction of an initial ensemble of particles falls in the accelerator-mode region, we expect the average value of P^2 to initially increase linearly with t as the bulk of the particles (i.e., those not in the accelerator mode) diffuse. However, eventually the contribution to the average of P^2 from the small number of large P value, accelerator-mode particles will become comparable to the contribution from the diffusing particles. After this time, the average should increase like t^2 (acceleration). Quantum effects allow particles to tunnel out of the accelerator-mode regions, and thus mitigate their effect. A simple model describing the diffusion, acceleration, and tunneling processes will be developed and its results compared with the results of the numerical solution to the full problem (Sec. V). Good agreement between the model and the numerical wave-function results is obtained.

One of the main motivations of this paper stems from the fact that tiny integrable regions in an otherwise predominantly ergodic phase space (e.g., the accelerator modes of the standard map) tend to invalidate or complicate attempts to build statistical descriptions of the classical dynamics of such systems. On the other hand, the corresponding quantum problem may be expected to be much less sensitive to tiny integrable phase-space regions of the classical problem, since such regions can be tun-

neled out of, or may not have any influence at all, if their area is of the order of $\hbar$ or smaller. Thus, over the early time, $(\Delta\omega)t \lesssim 1$, the statistical description of the dynamics may be more valid for the small-$\hbar$ quantum problem than for the corresponding classical problem. While the results of this paper cannot be said to have proven the general utility of this point of view, we believe that they do provide some measure of support for these arguments.

II. THE QUANTUM STANDARD MAP

The Hamiltonian for the kicked rotator is

$$H=\frac{P^2}{2I}-(I\omega_0^2\cos x)\bar{\delta}\left[\frac{t}{T}\right] , \qquad (2)$$

where x is an angular coordinate with period 2π, P is the angular momentum, I the moment of inertia, ω_0 the natural frequency of small oscillations, and $\bar{\delta}(t/T)$ is a periodic δ function with period T,

$$\bar{\delta}\left[\frac{t}{T}\right]=\sum_{j=-\infty}^\infty \delta\left[j-\frac{t}{T}\right] . \qquad (3)$$

The classical equations of motion are

$$\dot{P}=-I\omega_0^2\sin x\,\bar{\delta}\left[\frac{t}{T}\right] , \qquad (4)$$

$$\dot{x}=P/I . \qquad (5)$$

Using the notation

$$p_n=\lim_{\delta\to0^+} p(nT-\delta) , \qquad (6)$$

we can integrate the equations of motion to obtain

$$p_{n+1}=p_n-\epsilon\sin x_n , \qquad (7)$$

$$x_{n+1}=x_n+p_{n+1} , \qquad (8)$$

where $\epsilon=(\omega_0^2 T^2)$ and $p=PT/I$. This is the standard map.[2]

Schrödinger's equation is

$$i\hbar\frac{\partial\psi}{\partial t}=-\frac{\hbar^2}{2I}\frac{\partial^2\psi}{\partial x^2}-(I\omega_0^2\cos x)\bar{\delta}\left[\frac{t}{T}\right]\psi . \qquad (9)$$

Defining $\bar{t}=t/T$ and $\tau=\hbar T/I$, we obtain

$$i\tau\frac{\partial\psi}{\partial\bar{t}}=-\frac{\tau^2}{2}\frac{\partial^2\psi}{\partial x^2}-\epsilon\cos x\sum_n\delta(\bar{t}-n)\psi(x) . \qquad (10)$$

There are two independent parameters in the Schrödinger equation, ϵ and τ. The quantity ϵ is the independent parameter of the standard mapping, with $\epsilon\simeq1$ corresponding to the onset of stochasticity. For large ϵ, the quasilinear diffusion coefficient in p is $D\simeq\epsilon^2/2$ (see, for example, Ref. 5). The quantum parameter is τ, which is directly proportional to $\hbar$. The classical limit corresponds to $\tau\to0$.

Denote $\psi_{n\pm}(x)=\lim_{\delta\to0^\pm}\psi(x,\epsilon+\delta)$. Integrating over the delta function yields
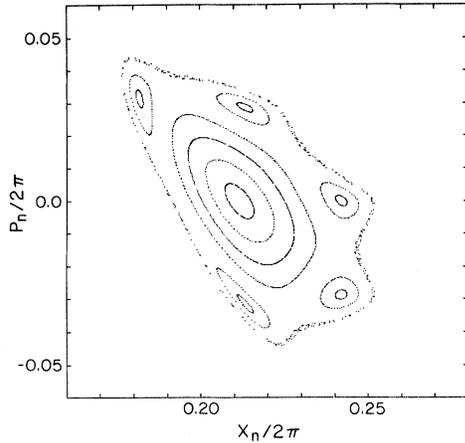
FIG. 1. Surface of section plot of an accelerator mode of the standard map with $\epsilon = 2\pi(1.03)$.

$$\psi_{n_+} = \psi_{n_-}\exp\left[i\left[\frac{\epsilon}{\tau}\right]\cos x\right] . \tag{11}$$

Since ψ is a periodic function of x, we can write

$$\hat{\psi}(l) = \frac{1}{2\pi}\int_0^{2\pi}\exp(ilx)\psi(x)dx , \tag{12}$$

$$\psi(x) = \sum_{l=-\infty}^{\infty}\exp(-ilx)\hat{\psi}(l) . \tag{13}$$

In the transform space, the free-particle propagation yields

$$\hat{\psi}_{(n+1)_-}(l) = \hat{\psi}_{n_+}(l)\exp\left[-\frac{i\tau l^2}{2}\right] . \tag{14}$$

III. NUMERICAL PROCEDURES

In what follows we shall be interested in numerically advancing the wave function forward in time. The algorithm used to propagate ψ one step forward is based on Eqs. (11)–(14). The wave function ψ is represented in the computer by a complex array A of length N. The subscript of A denotes the array element, the superscript denotes the time level:

$$A_j^{n_+} = \psi_{n_+}\left[\left[\frac{j-1}{N}\right]2\pi\right] . \tag{15}$$

First, a fast Fourier transformation is done,

$$A_j^{n_+} \rightarrow \hat{A}_j^{n_+} . \tag{16}$$

In the transform space, the free-particle propagation is accomplished by multiplying by a phase factor,

$$\hat{A}_j^{(n+1)_-} = \begin{cases} \hat{A}_j^{n_+}\exp[-i\tau(j-1)^2/2] , & 1 \leq j \leq \dfrac{N}{2} \\[2mm] \hat{A}_j^{n_+}\exp[-i\tau(j-1-N)^2/2] , & \dfrac{N}{2}+1 \leq j < N. \end{cases} \tag{17}$$

An inverse Fourier transform is performed,

$$\hat{A}_j^{(n+1)_-} \rightarrow A_j^{(n+1)_-} . \tag{18}$$

Finally, the effect of the potential is multiplication by a phase factor:

$$A_j^{(n+1)_+} = A_j^{(n+1)_-}\exp\left\{i\left[\frac{\epsilon}{\tau}\right]\cos\left[\left[\frac{j-1}{N}\right]2\pi\right]\right\} . \tag{19}$$

The numerical algorithm conserves the wave-function normalization to within about machine round-off per time step.

IV. ACCELERATOR MODES AND DIFFUSION FOR THE CLASSICAL MAP

An accelerator mode of a mapping is a stable region in which trajectories are continually accelerated. As an example, consider the trajectory of the initial point $(x_0,p_0) = (\pi/4,0)$ of the standard map with $\epsilon = 2\pi m$. The trajectory is easy to compute, and from Eqs. (7) and (8) we obtain

$$(x_n,p_n) = (\pi/4, -2\pi mn) = (\pi/4, -\epsilon n) .$$

(The x position is modulo 2π.) The angular momentum increases linearly in time. (x_0,p_0) is called an accelerating fixed point. Several accelerating fixed points have been cataloged for the standard map in Ref. 5. The region near a stable accelerating fixed point is an accelerator mode. Figure 1 is a surface of section plot of the accelerator mode near $x = \pi/4$, $\epsilon = 2\pi(1.03)$.

Accelerator modes are important in calculating the momentum-space diffusion coefficient. The diffusion coefficient is

$$D = \lim_{n\to\infty}\frac{\langle(p_n-p_0)^2\rangle}{2n} , \tag{20}$$

where the brackets denote an average over an ensemble of trajectories. If any member of the ensemble is located within an accelerator mode, $\langle(p_n-p_0)^2\rangle$ eventually increases faster than n for large n, and hence the limit does not exist. The diffusion coefficient is then undefined. In Ref. 5 the effects of noise are shown to remove this divergent behavior. If one limits the ensemble so that no ensemble trajectories are within accelerator modes, there can still be problems. In particular, a trajectory can spend a very long time in the "sticky region" near an accelerator mode, and thus be accelerated for an extremely long time
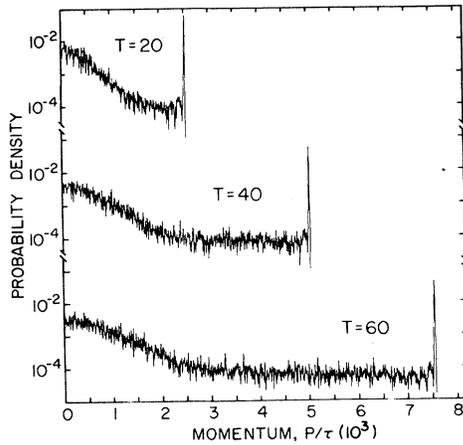
FIG. 2. Momentum-space probability distribution at three successive times with $\epsilon=2\pi(1.03)$ and $\tau=0.05$. Note the sharp peak of the accelerator mode which moves linearly (in momentum space) in time. Distribution is symmetric about $p=0$, and only positive momentum is shown. Momentum is a discrete variable. Distribution appears continuous because the points have been connected by straight lines.

before escaping. Karney has made a detailed study of this phenomenon.[15]

V. QUANTUM EFFECTS ON ACCELERATOR MODES AND DIFFUSION

We now turn to the quantum case. Figure 2 shows the momentum-space probability distribution function at three successive times. The ϵ value $[2\pi(1.03)]$ is such that classically there are two accelerator modes, accelerating in opposite directions. The initial state chosen was $\widehat{\psi}(l)=\delta_{l,0}$. The broad peak at $l=0$ is the diffusion of probability away from $l=0$. The sharp peaks at large l values are the accelerator modes. They propagate linearly in time. The plateau region between the accelerator mode and the $l=0$ peak we call the wake. It consists of proba-
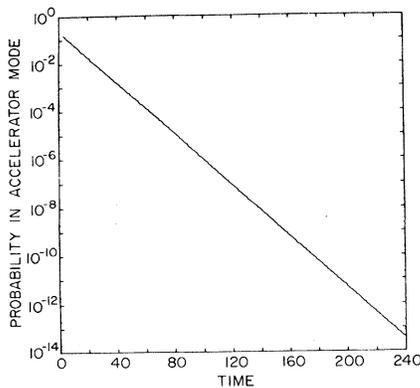
FIG. 3. Fraction of probability in an accelerator mode vs time, with $\epsilon=2\pi(1.03)$ and $\tau=0.1$. Exponential decay rate is $\gamma=0.123$.
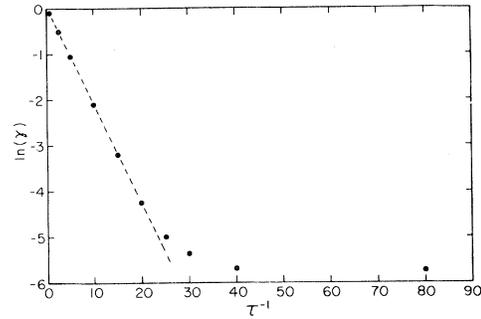
FIG. 4. Logarithm of the decay rate γ vs τ^{-1}. Straight section at low τ^{-1} (dashed line) indicates $\gamma\sim\exp(-\tau^{-1})$. At large τ^{-1} the map is more classical, and the sticky-region decay is important. $\epsilon=2\pi(1.03)$.

bility that has been lost by the accelerator mode as it propagated outward. Figure 3 shows the fraction of probability in one of the accelerator modes versus time. The plot is semilogarithmic, and it is clear that the probability ρ_a in the accelerator mode decays exponentially,

$$\rho_a(t)=\rho_a(0)\exp(-\gamma t) .\qquad(21)$$

For the case above, $\gamma=0.123$.

We interpret the exponential loss of probability from the accelerator mode as a barrier-penetration process. The probability is trapped within the accelerator mode, but slowly tunnels out.

For a continuous-time system, the WKB approximation is

$$\psi\sim\exp\left[-i\int_{x_0}^{x}k(x')dx'\right] ,\qquad(22)$$

where

$$k(x')=\frac{1}{\hbar}\{2m[E-V(x')]\}^{1/2}\qquad(23)$$

is the local wave vector. If there is a classically forbidden region between points x_1 and x_2, the transmission coefficient for penetrating this barrier is on the order of

$$\Gamma\sim\exp\left[\frac{-1}{\hbar}\int_{x_1}^{x_2}\{2m[V(x')-E]\}^{1/2}dx'\right] .\qquad(24)$$

In the discrete-time case we expect that the probability decay rate from the accelerator mode will have the same $\hbar$ dependence as the transmission coefficient in a continuous-time system. Since τ is directly proportional to $\hbar$, we expect

$$\gamma=\exp\left[\frac{-B}{\tau}\right]\qquad(25)$$

with B some constant.

Figure 4 is a plot of $\ln(\gamma)$ vs τ^{-1}. The prediction of Eq. (24) is quite accurate for large values of τ, but does not hold as τ gets very small. This is due to the sticky region. For τ small, the time evolution is close to classical, and the classical losses from the sticky region near the ac-
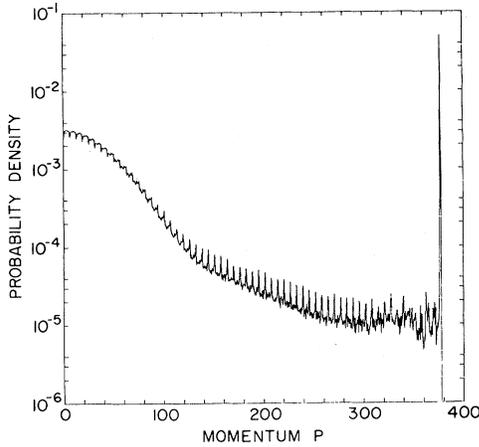
FIG. 5. Momentum distribution function for the classical map at $t=60$, $\epsilon=2\pi(1.03)$. Only positive momentum is shown.

celerator mode dominate the quantum barrier-penetration losses from the accelerator mode itself. Although the sticky-region losses are shown as exponential decay rate in Fig. (4), the observation time is smaller than $1/\gamma$. Thus, the sticky-region losses may well not be exponential.

The wake left by an accelerator mode consists of both sticky-region and barrier-penetration losses. In particular, the sticky-region losses show up as a wake in the classical case. Figure 5 shows a momentum-space distribution for the classical standard map, Eqs. (7) and (8). This plot was made by following a large number (10^7) of trajectories of the standard map with initial positions on the $p=0$ axis. The initial x positions were evenly distributed. After 60 iterations, the momenta of the trajectories were sorted and the distribution plotted. The accelerator mode and the wake are quite clear.

We now present a model that describes the gross features of the momentum-space probability distribution in the presence of accelerator modes. Consider the time evolution of the probability that is not located within the accelerator mode. Let f denote the probability distribution in momentum space. Our model equation is

$$\frac{\partial f}{\partial t} = D\frac{\partial^2 f}{\partial p^2} + S .$$ (26)

The first term on the right-hand side represents the diffusion of probability. The second term represents the tunneling from the accelerator modes:
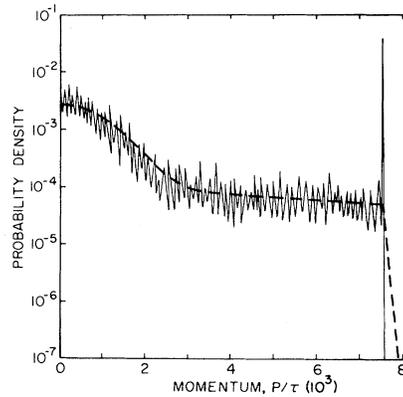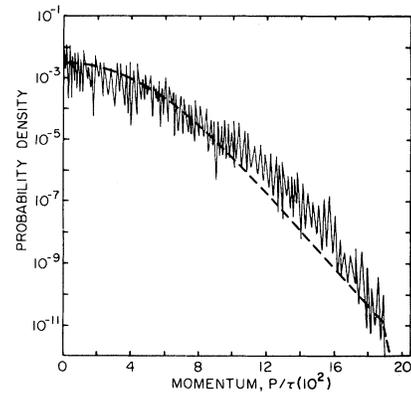
FIG. 6. Comparison of actual (solid) and predicted (dashed) momentum distribution function for (a) $\tau=0.2$ and (b) $\tau=0.05$. Solid curve has been redrawn, and some of the fine scale structure has been lost. Prediction is from Eq. (28), and does not include the probability in the accelerator mode itself. $\epsilon=2\pi(1.03)$, $t=60$.

$$S = \frac{\gamma N_0}{2}\exp(-\gamma t)[\delta(p-\epsilon t)+\delta(p+\epsilon t)] .$$ (27)

γ is the loss rate from the accelerator mode, and N_0 is the initial size of the two accelerator modes. The assumptions underlying Eq. (26) are that the initial probability not in the accelerator mode diffuses outward, and the probability that leaks out of an accelerator mode starts to diffuse after it leaks out. Using the Green function for the diffusion equation and the initial condition $f(p,0) = (1-N_0)\delta(p)$, the solution to Eq. (27) is

$$f(p,t) = \frac{(1-N_0)}{(4\pi Dt)^{1/2}}\exp\left[\frac{-p^2}{4Dt}\right] + \int_0^t dt'\left[\frac{\gamma N_0\exp(-\gamma t')}{2}\right]\frac{1}{[4\pi D(t-t')]^{1/2}}$$

$$\times\left[\exp\left[\frac{-(p-\epsilon t')^2}{4D(t-t')}\right] + \exp\left[\frac{-(p+\epsilon t')^2}{4D(t-t')}\right]\right] .$$ (28)
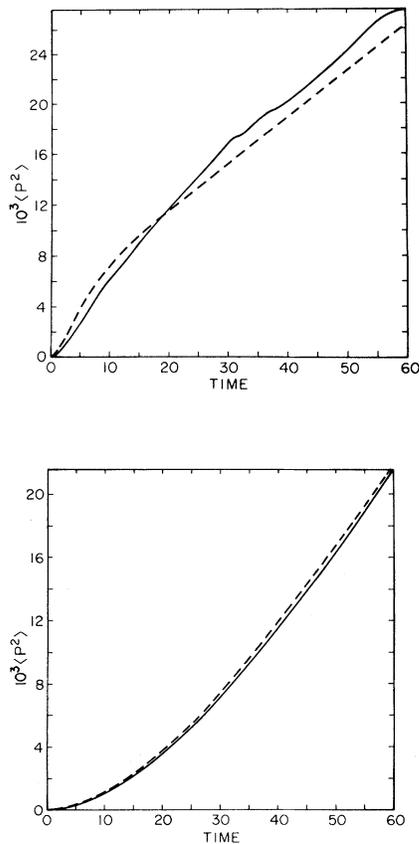
FIG. 7. Comparison of actual (solid) and predicted (dashed) mean square momentum vs time for (a) $\tau=0.2$ and (b) $\tau=0.05$. Prediction is from Eq. (29), with $\epsilon=2\pi(1.03)$.

Figure 6 shows plots of $f(p,t)$ along with the actual distribution function for two different values of τ. N_0 and γ are determined from the decay of the accelerator mode. The diffusion coefficient is that computed in Ref. 13, where the method of paths[4] was applied to the quantum Wigner function. The central diffusion peak and wake are apparent. [The accelerator mode is not present, since it is not included in f(p,t).] Also, there is a slight amount of probability predicted beyond the accelerator mode. This is the probability that has diffused faster than the accelerator mode propagates, and is an artifact of the

continuous-time (rather than discrete-time) nature of Eq. (26). Taking the second moment of the distribution of Eq. (28), and including the probability in the accelerator mode, we have

$$\langle p^2 \rangle = \langle p^2 \rangle_0 + 2\epsilon^2 N_0 \gamma^{-2} + 2DN_0[\exp(-\gamma t)-1]\gamma^{-1}$$
$$-2\epsilon^2 N_0 \exp(-\gamma t)\gamma^{-1}(t+\gamma^{-1})+2Dt \ . \quad (29)$$

Note that asymptotically, $\langle p^2 \rangle \propto t$. The leakage from the accelerator mode has eliminated the divergence in the diffusion coefficient. Plots of Eq. (29) compared with the actual $\langle p^2 \rangle$ are shown for two different values of τ in Fig. 7. From the results depicted in Figs. 6 and 7 we conclude that the model, Eq. (26), predicts the quantum behavior of the momentum distribution quite well.[16]

VI. CONCLUSION

For the classical kicked rotator with strong kicking, $\epsilon \gg 1$ in Eqs. (7) and (8), the phase space (p,x) is predominantly ergodic, and most initial conditions lead to diffusive particle behavior. However, for $\epsilon \cong 2\pi m$ where m is an integer, small integrable regions (called accelerator modes) appear within the predominantly ergodic phase space. Particles initialized within these regions accelerate rather than diffuse. If one considers an ensemble of initial conditions, with even a small fraction of the particles initialized in the accelerator-mode region, then in the long-time limit $\langle p^2 \rangle$ will become proportional to t^2 rather than to t. That is, the small number of accelerating particles eventually come to dominate the larger number of diffusing particles when one computes $\langle p^2 \rangle$. Here, we have considered the quantum effects on this problem. We find that, due to tunneling out of the accelerator-mode regions, their effect is reduced. A simple model for this process has been developed and compared with numerical solutions of the wave equation. Results from the model and the numerical solutions agree well. Based on these results, we speculate that problems (due to the possible presence of small integrable phase-space regions) in the application of statistical concepts to classical mechanics may, in some cases, be mitigated by quantum or finite-wavelength effects.

ACKNOWLEDGMENT

[1]A. J. Lichtenberg and M. A. Lieberman, *Regular and Stochastic Motion* (Springer, New York, 1983).
[2]B. V. Chirikov, Phys. Rep. 52, 265 (1979).
[3]J. Greene, J. Math. Phys. 9, 760 (1968); 20, 1183 (1979); D. F. Escande and F. Doveil, J. Stat. Mech. 26, 257 (1981); G. Schmidt, Phys. Rev. A 22, 2849 (1980); L. Kadanoff, Phys. Rev. Lett. 47, 1641 (1981).
[4]A. B. Rechester and R. B. White, Phys. Rev. Lett. 44, 1586 (1980); A. B. Rechester, R. B. White, and M. N. Rosenbluth, Phys. Rev. A 23, 2664 (1981); J. R. Cary, J. D. Meiss, and A. Bhattacharjee, *ibid.* 23, 2744 (1981); H. D. I. Abarbanel, Phy-

sica 4D, 89 (1981); T. M. Antonsen and E. Ott, Phys. Fluids 24, 1635 (1981).
[5]C. F. F. Karney, A. B. Rechester, and R. B. White, Physica 4D, 425 (1982).
[6]G. Casati, B. V. Chirikov, F. M. Izrailev, and J. Ford, in *Stochastic Behavior in Classical and Quantum Hamiltonian Systems*, edited by G. Casati and J. Ford (Springer, New York, 1979), p. 334.
[7]B. V. Chirikov, F. M. Izrailev, and D. L. Shepelyanski, Sov. Sci. Rev. C2, 209 (1981).
[8]F. M. Izrailev and D. L. Shepelyanski, Theor. Math. Phys. 43,

417 (1980).

[9]T. Hogg and B. A. Huberman, Phys. Rev. Lett. 48, 711 (1982).

[10]S. Fishman, D. R. Grempel, and R. E. Prange, Phys. Rev. Lett. 49, 509 (1982).

[11]M. V. Berry, J. Phys. A 10, 1083 (1977); M. V. Berry, N. L. Balazs, M. Tabor, and A. Voros, Ann. Phys. (N.Y.) 112, 26 (1979); S. W. McDonald and A. N. Kaufman, Phys. Rev. Lett. 42, 1189 (1979); J. S. Hutchinson and R. E. Wyatt, Chem. Phys. Lett. 72, 378 (1980); D. W. Noid, M. L. Koszykowski, and R. A. Marcus, J. Chem. Phys. 71, 2864 (1979); M. C. Gutzwiller, Physica 5D, 183 (1982).

[12]J-M. Wersinger, E. Ott, and J. M. Finn, Phys. Fluids 21, 2263 (1978); E. Ott, ibid. 22, 2246 (1979); P. T. Bonoli and E. Ott,

ibid. 25, 359 (1982); E. Ott and W. M. Manheimer, Phys. Rev. A 25, 1808 (1982); G. Casati and I. Guarneri, Phys. Rev. Lett. 50, 640 (1983).

[13]E. Ott, in Long Time Prediction in Dynamics, edited by C. W. Horton, Jr., L. E. Reichl, and V. B. Szebehely (Wiley, New York, 1983), p. 281.

[14]J. L. Lebowitz and O. Penrose, Physics Today 26 (2), 23 (1973).

[15]C. F. F. Karney, Physica, 8D, 360 (1983).

[16]Although it appears that accelerator modes do not lead to $\langle p^2 \rangle \propto t^2$ for the quantum case, quantum resonances (cf. Ref. 8) do give such behavior when $\tau = 4\pi r/q$, where r and q are relatively prime.